Progress In Electromagnetics Research B, Vol. 27, 151–163, 2011

THREE-DIMENSIONAL AXISYMMETRIC INVISIBILITY CLOAKS WITH ARBITRARY SHAPES IN LAYERED-MEDIUM BACKGROUND

Y. B. Zhai and T. J. Cui

State Key Laboratory of Millimeter Waves
Department of Radio Engineering
Southeast University
Nanjing 210096, China

Abstract—Three-dimensional (3D) axisymmetric invisibility cloaks with arbitrary shaped in layered-media background are presented using the transformation optics. The inner and outer boundaries of the cloaks can be non-conformal with arbitrary shapes, which considerably improve the flexibility of the cloaking applications. However, such kinds of 3D cloaks cannot be simulated using the commercial softwares due to the tremendous memory requirements and CPU time. By taking advantage of the rotationally symmetrical property, we propose an efficient finite-element method (FEM) to simulate and analyze the 3D cloaks, which can greatly reduce the CPU time and memory requirements. The method is based on the electric-field formulation, in which the transverse fields are expanded in terms of second-order edge-based vector basis functions and the azimuth components are expanded using second-order nodal-based scalar basis functions. The FEM mesh is truncated using the absorbing boundary condition. Excellent cloaking performance of the 3D cloaks in layered-media background has been verified by the proposed method.

1. INTRODUCTION

Controlling electromagnetic fields using material properties given by the optical transformation approach has recently drawn extensive attention in the scientific and engineering communities. The transformation properties of Maxwell's equations under certain coordinate transformations yield material properties that have

Received 15 August 2010, Accepted 25 November 2010, Scheduled 30 November 2010
Corresponding author: T. J. Cui (tjcui@seu.deu.cn).

interesting functionalities, such as invisibility cloaks [1–6], EM-wave concentrators [7, 8], rotators [9], and hyperlens [10, 11]. The invisibility cloak, due to its impressive applications, has received much more intensive study. Most of such researches have been focused on the case of homogeneous background (the free space). Recently, two-dimensional (2D) cylindrical cloaks with arbitrary shapes in layered media and in gradually changing media have been proposed analyzed in [12, 13].

In the study of various cloaks, the numerical simulation is an efficient way to verify the cloaking effects. The ray-tracing simulations [1, 2] supporting the conclusions by Pendry et al. [1] were reported in the geometric optics limit. The full-wave finite-element simulations [3] were performed to study the effects of cloaking material perturbations to the propagation of the incident waves in 2D cylindrical cases. A rigorous and modified solution to Maxwell's equations for a spherical cloak has been reported in [5, 6]. The discrete dipole approximation has been applied to simulate three-dimensional (3D) spherical cloaks and irregular 3D cloaks [14, 15]. One problem of the method is that it is difficult to get the accurate field inside the cloaked region for cloak with large tangential component of the refractive index because the DDA formalism is not applicable under this condition and the discrete array of dipoles can not sufficiently represent such inhomogeneous cloak [14]. Additionally, the full-wave analysis of large and complicated 3D cloaks are still limited due to the extremely large amount of computational burden and memory requirements.

The finite-element method (FEM) is a very flexible approach to study arbitrarily-shaped inhomogeneous and anisotropic dielectric objects, which has significant computational advantages [16, 17]. When the scatterer is a body of revolution (BOR), the problem can be efficiently solved using a 2D version of FEM by taking advantage of the rotationally symmetrical property [18, 19]. Based on such a method, rotational 3D cloaks and other metamaterial devices in free space have been analyzed [20].

In this paper, 3D axisymmetric invisibility cloaks with arbitrary shapes located in layered-media background are presented and designed using the transformation optics. The inner and outer boundaries of the cloaks can be non-conformal with arbitrary shapes, which considerably improve the flexibility of the cloaking applications. Such kinds of 3D cloaks cannot be simulated using the commercial softwares. Hence we propose an efficient FEM to simulate and analyze the 3D cloaks, which can greatly reduce the CPU time and memory requirements. In the method, the transverse fields are expanded in terms of second-order edge-based vector basis functions and the

azimuth components are expanded using second-order nodal-based scalar basis functions, which yields more accurate solutions since higher order polynomials give a better representation of a field for a given number of unknowns. The FEM mesh is truncated using the absorbing boundary condition, not the PML [18, 20]. That is because if PML is used to truncated the FEM mesh, the numerical result shows the computed scattering field expanded with second-order edge-based vector and nodal-based scalar basis functions is instable and singular near the inner boundary of the cloak where the permittivity and permeability of the cloak are singular. By the proposed method, excellent cloaking performance of the 3D cloaks in layered-media background has been verified.

2. FEM FORMULATIONS

We first consider a general scattering problem of BOR with arbitrarily inhomogeneous and anisotropic permittivity and permeability. According to the generalized variational principle [21], the functional of the problem is given by the following equation

$$F(\mathbf{E}) = \frac{1}{2}\iiint_V \left[(\nabla\times\mathbf{E})\cdot\bar{\bar{\mu}}_r^{-1}\cdot(\nabla\times\mathbf{E}) - k_0^2\mathbf{E}\cdot\bar{\bar{\epsilon}}_r\cdot\mathbf{E}\right]dV + \iint_S\left[\frac{jk_0}{2}(\hat{n}\times\mathbf{E})\cdot(\hat{n}\times\mathbf{E}) + \mathbf{E}\cdot\mathbf{U}^i\right]dS, \quad (1)$$

in which $k_0 = \omega\sqrt{\mu_0\varepsilon_0}$ is the free-space wavenumber, $\mathbf{U}^i = \hat{n}\times(\nabla\times\mathbf{E}^i) + jk_0\hat{n}\times(\hat{n}\times\mathbf{E}^i)$ is the known vector, that is based on the first-order absorbing boundary condition (ABC). $\mathbf{E}^i$ denotes the incident electric field in the background medium, which can be easily formulated for the plane-wave incidence [22]. $\bar{\bar{\mu}}_r$ and $\bar{\bar{\epsilon}}_r$ are the relative permittivity and permeability tensors of BOR, which have the following symmetrical forms

$$\bar{\bar{\epsilon}}_r = \begin{pmatrix}\epsilon_{\rho\rho} & 0 & \epsilon_{\rho z}\\ 0 & \epsilon_{\phi\phi} & 0\\ \epsilon_{\rho z} & 0 & \epsilon_{zz}\end{pmatrix}, \qquad \bar{\bar{\mu}}_r = \begin{pmatrix}\mu_{\rho\rho} & 0 & \mu_{\rho z}\\ 0 & \mu_{\phi\phi} & 0\\ \mu_{\rho z} & 0 & \mu_{zz}\end{pmatrix}. \quad (2)$$

To take the advantage of the rotational symmetry of the problem, the fields are expanded in the Fourier modes as [18]:

$$\mathbf{E} = \sum_{m=-\infty}^{+\infty}\left[\mathbf{E}_{t,m}(\rho,z) + \hat{\phi}E_{\phi,m}(\rho,z)\right]e^{jm\phi}, \quad (3)$$

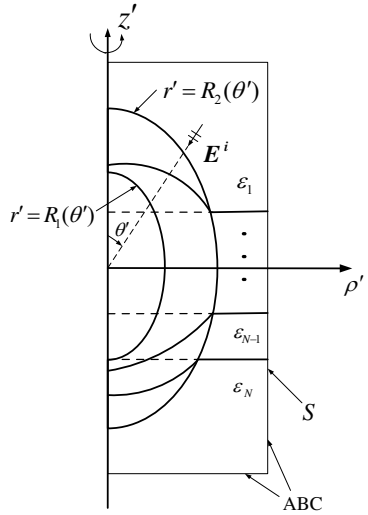

Figure 1. The slice of a 3D cloak embedded in N-layered media with ABC. The cloaking shell exists in the region defined by $R_1(\theta') < r' < R_2(\theta')$. The layer interfaces inside the cloak become curves described by (17).

in which the unknown fields are expanded as

$$E_{\phi,0} = \sum_{i=1}^{6} e^e_{\phi,i} N^e_i, \qquad \mathbf{E}_{t,0} = \sum_{i=1}^{8} e^e_{t,i} \mathbf{N}^e_i \tag{4}$$

for $m = 0$;

$$E_{\phi,\pm1} = \sum_{i=1}^{6} e^e_{\phi,i} N^e_i, \qquad \mathbf{E}_{t,\pm1} = \mp j\hat{\rho} E_{\phi,\pm1} + \sum_{i=1}^{8} \left[e^e_{t,i} \rho \mathbf{N}^e_i \right] \tag{5}$$

for $m = \pm 1$; and

$$E_{\phi,m} = \sum_{i=1}^{6} e^e_{\phi,i} N^e_i, \qquad \mathbf{E}_{t,m} = \sum_{i=1}^{8} e^e_{t,i} \rho \mathbf{N}^e_i \tag{6}$$

for $|m| > 1$. Here,

$$\begin{array}{lll} N^e_1 = \xi, & N^e_2 = \eta, & N^e_3 = \gamma \\ N^e_4 = 4\xi\eta, & N^e_5 = 4\eta\gamma, & N^e_6 = 4\gamma\xi \end{array} \tag{7}$$

$$\begin{array}{ll} \mathbf{N}^e_1 = \xi\nabla_t\eta - \eta\nabla_t\xi, & \mathbf{N}^e_2 = \eta\nabla_t\gamma - \gamma\nabla_t\eta \\ \mathbf{N}^e_3 = \gamma\nabla_t\xi - \xi\nabla_t\gamma, & \mathbf{N}^e_4 = (\xi - \eta)\mathbf{N}^e_1 \\ \mathbf{N}^e_5 = (\eta - \gamma)\mathbf{N}^e_2, & \mathbf{N}^e_6 = (\gamma - \xi)\mathbf{N}^e_3 \\ \mathbf{N}^e_7 = \gamma\mathbf{N}^e_1, & \mathbf{N}^e_8 = \xi\mathbf{N}^e_2. \end{array} \tag{8}$$

Equations (7) and (8) are the second-order hierarchical scalar shape functions [23] and vector shape functions [24], respectively. ξ, η and γ are called as area coordinates [21], and $\xi + \eta + \gamma = 1$. Substituting the expansions (3) into (1), the functional is differentiated with respect to the unknown coefficients, and then the result is set to zero. This process yields a sparse and symmetric matrix equation:

$$\begin{pmatrix} A_{tt}^m & A_{t\phi}^m \\ A_{\phi t}^m & A_{\phi\phi}^m \end{pmatrix} \begin{pmatrix} e_t^m \\ e_\phi^m \end{pmatrix} = \begin{pmatrix} B_t^m \\ B_\phi^m \end{pmatrix}, \quad m = 0, \pm 1, \pm 2, \ldots. \tag{9}$$

The FEM matrix for a given mode number m is stored compactly and the matrix equation can be solved according the techniques described in Ref. [25]. The solution for each negative mode ($m < 0$) is simply related to that of the corresponding positive mode ($m > 0$) [18]. Hence the solutions need to be computed for the nonnegative modes only ($m = 0, 1, 2, \ldots$).

3. DESIGN OF 3D CLOAKS IN LAYERED-MEDIA BACKGROUND

Based on the form-invariant and spatial coordinate transformations of the Maxwell's equations, the permittivity and permeability tensors in the transformation media are derived as [2, 12]

$$\begin{aligned} \epsilon^{i'j'} &= \left|\det\left(\Lambda_i^{i'}\right)\right|^{-1} \Lambda_i^{i'} \Lambda_j^{j'} \epsilon^{ij}, \\ \mu^{i'j'} &= \left|\det\left(\Lambda_i^{i'}\right)\right|^{-1} \Lambda_i^{i'} \Lambda_j^{j'} \mu^{ij}, \end{aligned} \tag{10}$$

where, $\Lambda_\alpha^{\alpha'}$ is the Jacobian transformation matrix

$$\Lambda_\alpha^{\alpha'} = \frac{\partial x^{\alpha'}}{\partial x^\alpha}. \tag{11}$$

For inhomogeneous media, ϵ^{ij} and μ^{ij} are expressed in the form of

$$\begin{aligned} \epsilon^{ij} &= \epsilon^{ij}(x^\alpha), \\ \mu^{ij} &= \mu^{ij}(x^\alpha). \end{aligned} \tag{12}$$

Using $x^\alpha = f(x^{\alpha'})$, the transformation media are then expressed in the transformed space as

$$\begin{aligned} \epsilon^{i'j'} &= \left|\det\left(\Lambda_i^{i'}\right)\right|^{-1} \Lambda_i^{i'} \Lambda_j^{j'} \epsilon^{ij} \left(f\left(x^{\alpha'}\right)\right), \\ \mu^{i'j'} &= \left|\det\left(\Lambda_i^{i'}\right)\right|^{-1} \Lambda_i^{i'} \Lambda_j^{j'} \mu^{ij} \left(f\left(x^{\alpha'}\right)\right). \end{aligned} \tag{13}$$

For a transformation which compresses a spherical volume defined by $r < R_2(\theta)$ in the original space into an annular volume defined by $R_1(\theta') < r' < R_2(\theta')$ in the transformed space, the coordinate transformation can be generally defined as:

$$r' = R_1(\theta) + \frac{R_2(\theta) - R_1(\theta)}{R_2(\theta)} r, \quad \theta' = \theta, \quad \phi' = \phi \tag{14}$$

where (r, θ, ϕ) and (r', θ', ϕ') represent the spherical coordinates in the original and the transformed spaces, respectively. The transformed space is schematically illustrated in Fig. 1. Here, let us consider the situation where the background is composed of N isotropic layers with permittivities $\epsilon_1, \epsilon_2, \ldots, \epsilon_N$, and interfaces located at $z = d_1, d_2, \ldots, d_N$. The permittivity and the permeability of the original space can thus be written as

$$\epsilon(z) = \epsilon_1 + \sum_{n=1}^{N-1} (\epsilon_{n+1} - \epsilon_n) \mathrm{sgn}(d_n - z), \quad \mu = \mu_0, \tag{15}$$

where $\mathrm{sgn}(x)$ is defined as

$$\mathrm{sgn}(x) = \begin{cases} 0 & (x < 0) \\ 1 & (x > 0) \end{cases}. \tag{16}$$

Evidently, because the background is composed of N layered media, the cloak is divided into N parts by the interfaces, which become curves inside the cloak as described as the following function

$$z' = \frac{R_2(\theta') - R_1(\theta')}{R_2(\theta')} \frac{r'}{r' - R_1(\theta')} d_n, \quad n = 1, 2, \ldots, N. \tag{17}$$

From the above transformation equations, the permittivity and permeability tensors in the transformed space are derived in the cylindrical coordinates as

$$\begin{aligned} \overline{\overline{\epsilon}}'_r &= \left[\epsilon_1 + \sum_{n=1}^{N-1} (\epsilon_{n+1} - \epsilon_n) \, \mathrm{sgn}\left(d_n - \frac{z' R_2(\theta')}{R_2(\theta') - R_1(\theta')} \frac{r' - R_1(\theta')}{r'} \right) \right] \\ &\quad \times \begin{pmatrix} \chi_{\rho'\rho'} & 0 & \chi_{\rho' z'} \\ 0 & \chi_{\phi'\phi'} & 0 \\ \chi_{z'\rho'} & 0 & \chi_{z'z'} \end{pmatrix}, \end{aligned} \tag{18}$$

$$\overline{\overline{\mu}}'_r = \mu_0 \begin{pmatrix} \chi_{\rho'\rho'} & 0 & \chi_{\rho' z'} \\ 0 & \chi_{\phi'\phi'} & 0 \\ \chi_{z'\rho'} & 0 & \chi_{z'z'} \end{pmatrix}, \tag{19}$$

where

$$\chi_{\rho'\rho'} = \frac{(r' - R_1(\theta'))^2}{r'^2 R_3(\theta')} \sin^2(\theta') + \frac{(R_4 \sin(\theta') + r' \cos(\theta'))^2}{r'^2 R_3(\theta')}, \quad (20)$$

$$\begin{aligned} \chi_{\rho'z'} &= \chi_{z'\rho'}, \\ &= \frac{(r' - R_1(\theta'))^2}{r'^2 R_3(\theta')} \sin(\theta')\cos(\theta') \\ &\quad + \frac{(R_4 \sin(\theta') + r' \cos(\theta'))(R_4 \cos(\theta') - r' \sin(\theta'))}{r'^2 R_3(\theta')}, \end{aligned} \quad (21)$$

$$\chi_{\phi'\phi'} = \frac{1}{R_3(\theta')}, \quad (22)$$

$$\chi_{z'z'} = \frac{(r' - R_1(\theta'))^2}{r'^2 R_3(\theta')} \cos^2(\theta') + \frac{(R_4 \cos(\theta') - r' \sin(\theta'))^2}{r'^2 R_3(\theta')}, \quad (23)$$

and $R_3(\theta') = \frac{R_2(\theta') - R_1(\theta')}{R_2(\theta')}$, $R_4 = \frac{dR_1(\theta')}{d\theta'} + \frac{dR_3(\theta')}{d\theta'} \frac{r' - R_1(\theta')}{R_3(\theta')}$.

We remark that $R_1(\theta)$ and $R_2(\theta)$ can be chosen as closed contours with arbitrary shapes, which can be generally expressed by a Fourier series with periodic π. Hence (18)–(23) give the general and explicit expressions of the material parameters for 3D axisymmetric invisibility cloaks with arbitrary nonconformal cross section boundaries, which can make objects invisible in the layered-media background.

4. FULL-WAVE SIMULATIONS OF 3D AXISYMMETRICAL INVISIBILITY CLOAKS

3D invisibility cloaks in the layered-media background are simulated using the presented FEM method when illuminated by plane waves. The electric fields near the cloaks are calculated by (3), and their far-field radar cross sections (RCSs) are computed from the near-field values. It is assumed that the frequency of incident plane waves is 3 GHz. All computations are performed using a personal computer (Dell OptiPlex 960 with intel 3 GHz processor).

We consider a 3D cloak with complicated inner and the outer boundaries, whose contour equations are described by

$$\begin{aligned} R_1(\theta) &= 0.2 + 0.05\cos(3\theta) + 0.01\cos(\theta), \\ R_2(\theta) &= 0.35 + 0.03\cos(4\theta) - 0.02\cos(7\theta). \end{aligned} \quad (24)$$

The plane wave is incident to the interface located at $d_1 = 0$ m from the free space down to the lossy medium with the relative permittivities $\epsilon_{r2} = 2.0 - j0.2$. The cloaked region is free space. Fig. 2 shows the electric field distributions near the cloak in the xoz plane when the incident angle is 0° and 30°, respectively. From the figure, it is

seen that the scattering in the lossy medium background is almost unchanged when the the cloak is embedded. It takes about 620 MB memory and 18 minutes to compute the near fields when the incident angle is 30°.

Sometimes we are only able to cover the object with half of the cloak shell. For instance, if we want to hide a building on the ground, we might only be able to cover the part above the ground [12]. Fig. 3 shows the near field distributions with only the half of the cloak shell and Fig. 4 gives the corresponding bistatic RCS. We can find that if the ground cannot be considered as a PEC, i.e., significant reflection and transmission occurs at the interface, the scattering from the half of the shell is very large.

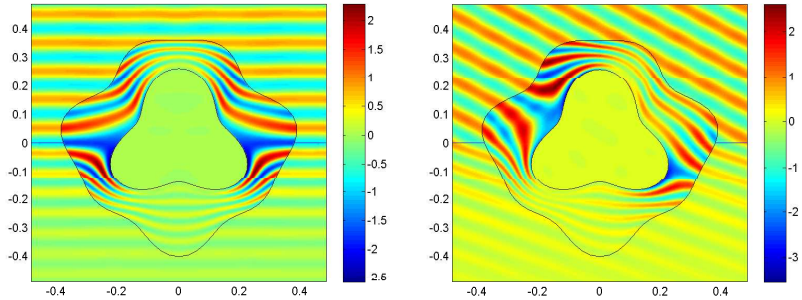

Figure 2. (color online) The real parts of the electric fields E_x for a 3D cloak in the xoz plane when the plane wave is illuminated. (a) The incident angle is 0°. (b) The incident angle is 30°.

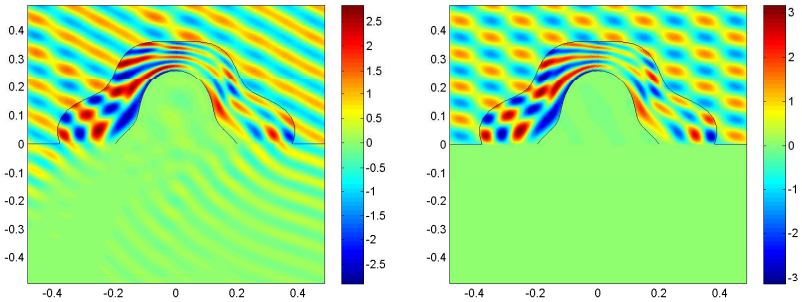

Figure 3. (color online) The real parts of the electric fields E_x for half of a 3D cloak in the upper half space (air) and lower half space (earth medium) when the plane wave is incident obliquely. (a) The earth medium is lossy medium with $\epsilon_{r2} = 2 - j0.2$. (b) The earth medium is PEC.

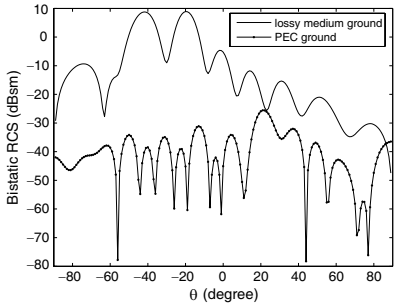

Figure 4. The bistatic RCSs for half of a 3D cloak in the upper half space (air) and lower half space (earth medium) when the plane wave is incident obliquely.

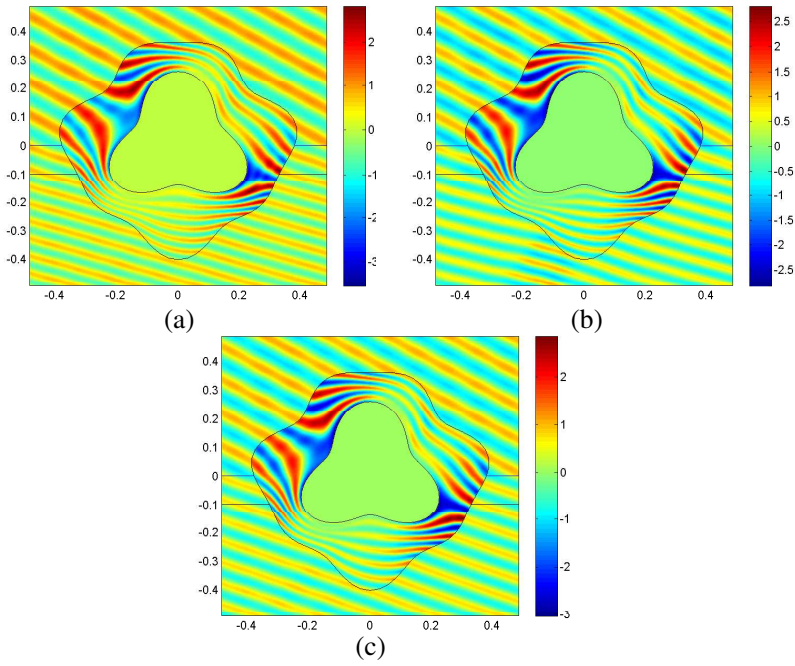

Figure 5. (color online) The real parts of the electric fields E_x for a 3D cloak in the xoz plane when the plane wave is incident obliquely. (a) Three-layered media with $\epsilon_{r1} = 1$, $\epsilon_{r2} = 2$, and $\epsilon_{r3} = 3$ and the interface located at $z = -0.1$ m is a curve line inside the cloak. (b) Three-layered media with $\epsilon_{r1} = 1$, $\epsilon_{r2} = 2$, and $\epsilon_{r3} = 3$ and the interface located at $z = -0.1$ m is a straight line inside the cloak. (c) Three-layered media with $\epsilon_{r1} = 1$, $\epsilon_{r2} = 2$, and $\epsilon_{r3} = 2.1$ and the interface located at $z = -0.1$ m is a straight line inside the cloak.

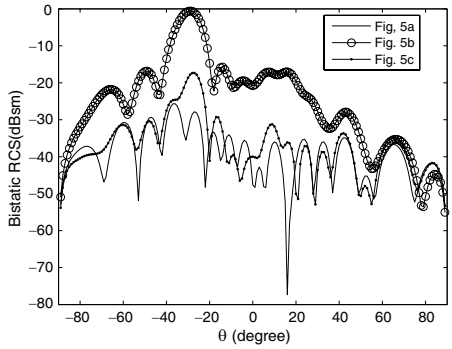

Figure 6. The bistatic RCSs for a 3D cloak in three layered media when the plane wave is incident obliquely.

Next, the above cloak with PEC filled is set in the three layered medium. The relative permittivities are $\epsilon_{r1} = 1$, $\epsilon_{r2} = 2$, and $\epsilon_{r3} = 3$ from top to bottom, and the two interfaces are located at $z = 0\,\mathrm{m}$ and $z = -0.1\,\mathrm{m}$. If the interface is not located at the plane $z = 0$, the interface inside the cloak should follow a curve described by (17) in order to guide the wave smoothly into another media in its original path. In Fig. 5(a), the interface located at $z = -0.1\,\mathrm{m}$ is no longer a straight line inside the cloak, the scattering is low and the RCS is very small shown in Fig. 6. If a straight interface is still used inside the cloak, the scattering increases dramatically. However, if the relative permittivities of the background does not vary obviously such as $\epsilon_{r2} = 2$, and $\epsilon_{r3} = 2.1$, a straight interface inside the cloak will not introduce very large scattering, as is shown in Fig. 5(b), Fig. 5(c) and Fig. 6.

5. CONCLUSIONS

In this work, 3D axisymmetric invisibility cloaks with arbitrary shapes in layered-media background are presented and designed using the optical transformation, and are simulated accurately using a specially designed FEM. The inner and outer boundaries of the cloaks can be non-conformal with arbitrary shapes. The near electric-field distributions and the far-field RCSs of 3D layered cloaks is computed and the applications of different cases in practical situations are discussed.

ACKNOWLEDGMENT

This work was supported in part by a Major Project of the National Science Foundation of China under Grant Nos. 60990320 and 60990324, in part by the National Science Foundation of China under Grant Nos. 60671015, 60871016, 60802001, and 60901011, in part by the Natural Science Foundation of Jiangsu Province under Grant No. BK2008031, and in part by the 111 Project under Grant No. 111-2-05.

REFERENCES

1. Pendry, J. B., D. Schurig, and D. R. Smith, "Controlling electromagnetic fields," *Science*, Vol. 312, No. 5781, 1780–1782, 2006.
2. Schurig, D., J. B. Pendry, and D. R. Smith, "Calculation of material properties and ray tracing in transformation media," *Opt. Express*, Vol. 14, 9794–9804, 2006.
3. Cummer, S. A., B. I. Popa, D. Schurig, D. R. Smith, and J. B. Pendry, "Full-wave simulations of electromagnetic cloaking structures," *Phys. Rev. E*, Vol. 74, 2006.
4. Schurig, D., J. J. Mock, B. J. Justice, S. A. Cummer, J. B. Pendry, A. F. Starr, and D. R. Smith, "Metamaterial electromagnetic cloak at microwave frequencies," *Science*, Vol. 314, 977–980, 2006.
5. Chen, H., B. I. Wu, B. Zhang, and J. A. Kong, "Electromagnetic wave interactions with a metamaterial cloak," *Phys. Rev. Lett.*, Vol. 99, 2007.
6. Andrey, N., W. Q. Cheng, and S. Zouhdi, "Transformation-based spherical cloaks designed by an implicit transformation-independent method: Theory and optimization," *New J. Phys.*, Vol. 11, 2009.
7. Luo, Yu., H. S. Chen, J. J. Zhang, L. Ran, and J. A. Kong, "Design and analytically full-wave validation of the invisibility cloaks, concentrators, and field rotators created with a general class of transformations," *Phys. Rev. B.*, Vol. 77, 2008.
8. Rahm, M., D. Schurig, D. A. Roberts, S. A. Cummer, D. R. Smith, and J. B. Pendry, "Design of electromagnetic cloaks and concentrators using form-invariant coordinate transformations of Maxwell's equations," *Photo. Nanos. Fund. Appl.*, Vol. 6, 87–95, 2008.
9. Chen, H. and C. T. Chan, "Transformation media that rotate electromagnetic fields," *Appl. Phys. Lett.*, Vol. 90, 2007.

10. Tsang, M. and D. Psaltis, "Magnifying perfect lens and superlens design by coordinate transformation," *Phys. Rev. B*, Vol. 77, 2008.
11. Kildishev, A. V. and E. E. Narimanov, "Impedance-matched hyperlens," *Opt. Lett.*, Vol. 32, 3432–3434, 2007.
12. Zhang, J. J., F. Huang, T. Jiang, Y. Luo, H. S. Chen, J. A. Kong, and B. I. Wu, "Cloak for multilayered and gradually changing media," *Phys. Rev. B*, Vol. 77, 2008.
13. Li, C., K. Yao, and F. Li, "Invisibility cloaks with arbitrary geometries for layered and gradually changing backgrounds," *J. Phys. D: Appl. Phys.*, Vol. 42, 2009.
14. You. Y., G. W. Kattawar, P. W. Zhai, and P. Yang, "Zero-backscatter cloak for aspherical particles using a generalized DDA formalism," *Opt. Express*, Vol. 16, 2068–2079, 2008.
15. You, Y., G. W. Kattawar, P. W. Zhai, and P. Yang, "Invisibility cloaks for irregular particles using coordinate transformations," *Opt. Express*, Vol. 16, 6134–6145, 2008.
16. Ping, X. W., T. J. Cui, and W. B. Lu, "The combination of Bcgstab with multifrontal algorithm to solve Febi-MLFMA linear systems arising from inhomogeneous electromagnetic scattering problems," *Progress In Electromagnetics Research*, Vol. 93, 91–105, 2009.
17. Sun, X. Y. and Z. P. Nie, "Vector finite element analysis of multicomponent induction response in anisotropic formations," *Progress In Electromagnetics Research*, Vol. 81, 21–39, 2008.
18. Greenwood, A. D. and J. M. Jin, "A novel efficient algorithm for scattering from a complex BOR using mixed finite elements and cylindrical PML," *IEEE Trans. Antennas Propgat.*, Vol. 47, 1260–1266, 1999.
19. Ding. D. Z. and R. S. Chen, "Electromagnetic scattering by conducting bodies of revolution (BOR) coated with homogeneous chiral media above a lossy half-space," *Progress In Electromagnetics Research*, Vol. 104, 385–401, 2010.
20. Zhai, Y. B., X. W. Ping, W. X. Jiang, and T. J. Cui, "Finite-element analysis of three-dimensional axisymmetrical invisibility cloaks and other metamaterial devices," *Commun. Comput. Phys.*, Vol. 8, 823–834, 2010.
21. Jin, J. M., *The Finite Element Method in Electromagnetics*, Wiley, New York, 1993.
22. Chew, W. C., *Waves and Fields in Inhomogeneous Media*, Van Nostrand Reinhold, New York, 1990.
23. Webb, J. P. and S. McFee, "The use of hierarchical triangles in

finite-element analysis of microwave and optical devical," *IEEE Transactions on Magnetics*, Vol. 27, 4040–4043, 1991.

24. Andersen, L. S. and J. L. Volakis, "Development and application of a novel class of hierarchical tangential vector finite elements for electromagnetics," *IEEE Trans. Antennas Propagat.*, Vol. 47, 112–120, 1999.
25. Chen, R. S., D. X. Wang, E. K. N. Yung, and J. M. Jin, "Application of the multifrontal method to the vector FEM for analysis of microwave filters," *Microw. Opt. Tech. Lett.*, Vol. 31, 465–470, 2001.